Dielectric Non-Linearity in Hard Piezoelectric Ceramics

D.A. Hall, P.J. Stevenson and T.R. Mullins*

Materials Science Centre, University of Manchester/UMIST, Manchester M1 7HS.
*DRA (Holton Heath), Poole, Dorset BH16 6JU.

Abstract

Dielectric properties of hard PZT (Lead Zirconate Titanate) ceramics were characterised using a variety of measurement methods and with field strengths in the range 100 to 1000 V mm^{-1}. Under high electric drive levels, the material was found to exhibit increasing dielectric non-linearity and loss as a result of hysteretic ferroelectric domain wall motion. High voltage bridge measurements indicated that the real part of permittivity ε_r' increased from 1270 to 1640 (i.e. by a factor of 1.3) as the electric field was increased to 500 V mm^{-1}, while the dielectric loss tan δ increased by a factor of 10, from 0.003 to 0.036. P-E (polarisation-electric field) measurements yielded similar values for the dielectric coefficients, as well as giving further insight into the stability of the remanent polarisation under these drive conditions. Fourier analysis of the current and voltage waveforms was also investigated as an alternative method of determining the dielectric parameters and providing a means of quantifying the degree of dielectric non-linearity.

1. Introduction

Piezoelectric materials have been employed for many years as electro-mechanical sensors and actuators, as acoustic sources, and for various types of electrical signal processing functions (e.g. resonators, filters)[(1)]. Novel applications are also being pursued in areas such as resonant sensors and active vibration control[(2)].

Conventional piezoelectric sensors generally make use of so-called 'soft' piezoelectric materials typified by donor-doped PZT (lead zirconate titanate) ceramics[3]. In these materials, the ferroelectric domain walls are relatively mobile under the influence of moderate electric fields, giving rise to a low coercive field (e.g. E_c = 0.8 kV mm^{-1}) and relatively high piezoelectric and dielectric coefficients (e.g. ε_r = 2900, tanδ = 0.027, d_{33} = 530 pC N^{-1})[4]. Similar materials are used in many types of piezoelectric actuators, as used for example in micropositioning. In these applications, non-linearity and hysteresis are clearly evident in the strain-field relationship and have to be accommodated in the overall device design[5].

In contrast, 'hard' PZT ceramics are commonly used in applications demanding high acoustic power densities e.g. ultrasonic cleaning and machining, piezoelectric motors, and SONAR transmitters. These materials are modified with acceptor dopants (e.g. Fe, Mn), which are thought to 'pin' the ferroelectric domain walls as a result of the gradual re-orientation of acceptor ion - oxygen vacancy defect dipoles in the same direction as that of the local domain polarisation[6,7]. Hard PZT ceramics generally exhibit reduced dielectric and piezoelectric coefficients (e.g. ε_r = 1300, tan δ = 0.003, d_{33} = 275 pC N^{-1}) and good stability under high levels of electrical and mechanical stress.

The present work was initiated in order to provide an improved understanding of the behaviour of such hard PZT ceramics under high drive conditions, with particular regard to their use in low-frequency (~ 1 kHz) SONAR transmitters. At present, the maximum electric drive levels are typically in the range 400 to 800 V mm^{-1} [8]; to date, there have been few studies of the factors affecting the maximum allowable drive limits in practical transducers, or of the materials degradation characteristics under such conditions.

The present paper describes the results of an initial investigation into dielectric non-linearity and hysteresis in hard PZT ceramics in the low to medium field region (100 to 1000 V mm^{-1}), since this provides a useful indication of the increasing dielectric and electro-mechanical losses which ultimately lead to degradation and electrical breakdown. The paper compares three different methods for characterising non-linear dielectric behaviour under high field conditions and proposes a means of monitoring the increasing dielectric non-linearity and loss in practical transducers.

2. Experimental Procedures

A set of poled, well aged hard PZT ceramics, type PZ26, were obtained from Ferroperm Ltd. (Hejreskovvej, DK-3490, Denmark) for use in the tests. The materials, supplied in the form of 10 mm diameter, 1 mm thick discs, were based on a tetragonal lead zirconate-lead titanate solid solution with a composition close to the morphotropic phase boundary[3]. A small amount of manganese was incorporated within the composition in order to yield the required hard piezoelectric behaviour. Typical properties of this material, as given by the manufacturer, are listed in Table 1. A Wayne-Kerr B6425 LCR meter in combination with a wire-wound alumina tube furnace was used to determine the low-field dielectric properties and the Curie temperature T_c, by heating up to a temperature of 500 °C under an electric field of 1 V mm^{-1}. XRD scans (made using a Philips PW 3020 diffractometer) were employed to determine the degree of tetragonality of the material.

A custom-built high voltage capacitance bridge based on a modified Schering bridge circuit (fig. 1) was used for measurement of the equivalent parallel capacitance C_p and resistance R_p of the specimens. In these measurements, the frequency of the test signal was 1 kHz and the equipment was able to apply fields up to 500 V mm^{-1}. The use of higher voltages was found to lead to dielectric breakdown, due to the relatively high power dissipation and therefore self-heating at this frequency. The real part of dielectric permittivity ε_r' was calculated from C_p according to the standard parallel plate capacitor equation, while the dielectric loss tan δ was derived from the parallel equivalent circuit as follows :

$$\tan\delta = \frac{1}{\omega C_p R_p} \qquad (1)$$

The imaginary part of the dielectric permittivity ε_r" was then calculated as the product of ε_r' and tan δ.

Polarisation-electric field measurements were carried out within a temperature controlled silicone oil bath using a computer-controlled Thurlby-Thandar TG1304 function generator in combination with a HVA1B high voltage (± 5 kV mm^{-1}) amplifier (Chevin Research, Otley, UK). Sinusoidal voltage waveforms at a frequency of 1 Hz were applied to the test samples, the resulting current being converted to a measurable voltage signal by means of a custom

built I-V converter incorporating an operational amplifier in a 'virtual earth' configuration. The applied electric field and resulting current waveforms were logged using a PC via an Amplicon PC226 12-bit A-D card. Numerical integration of the current waveform yielded the polarisation, thus enabling construction of the I-E and P-E loops. A schematic illustration of the measurement system is shown in fig. 2(a), while a more detailed diagram of the current-voltage converter is presented in fig. 2(b).

The instantaneous current I flowing through the specimen was calculated from the output voltage V_{out} and the standard reference resistor R_{st} as follows :

$$I = \frac{V_{out}}{R_{st}} \tag{2}$$

It was also found necessary to include a capacitor C_{st} (typically in the range 100 pF to 10 nF) in the I-V converter in order to suppress high frequency noise, the effective time constant of the circuit being given by $C_{st}R_{st}$ (typically around 10 ms). The dielectric permittivity was determined from the average gradient of the P-E loop :

$$\varepsilon_r^{'} = \frac{P_{\max}}{\varepsilon_0 E_0} \tag{3}$$

while the effective loss tangent was found from the hysteresis loss (i.e. the loop area) according to equation 4 [9] :

$$U_H = \pi \varepsilon_0 \varepsilon_r^{'} E^2 \tan\delta \tag{4}$$

The current and voltage waveforms recorded using the circuit described above were analysed further by means of a commercial data acquisition and signal processing package ('Signal Centre', Amplicon Liveline Ltd, Brighton, UK) in order to determine the Fourier components and phase relationship. The dielectric permittivity was derived from the magnitudes of the fundamental components of the voltage and current waveforms :

$$C = \frac{I_0}{V_0} . \frac{t}{A\varepsilon_0 \omega} \tag{5}$$

while the dielectric loss angle δ was found from the phase angle ϕ between I and V :

$$\delta = \frac{\pi}{2} + \phi \tag{6}$$

3. Results and Discussion

3.1. Structural Characterisation and Low Field Dielectric Measurements

Dielectric property measurements made using the conventional LCR bridge gave a good correlation with the manufacturer's data at room temperature, with both ε_r' and tan δ increasing gradually as the temperature was increased to 250 °C, as shown in fig. 3. Maxima in ε_r' and tan δ were evident at a temperature of approximately 345 °C, corresponding to the ferroelectric Curie temperature T_c. The pronounced increase in loss above T_c is related to the increase in electronic conductivity at high temperatures[10].

XRD analysis at room temperature indicated that the material was a tetragonal perovskite-type solid solution with a c/a ratio of approximately 1.022. Therefore, it can be concluded that the maxima in ε_r' and tan δ at T_c correspond to the phase transition from the high temperature cubic (paraelectric) phase to the low temperature tetragonal (ferroelectric) phase and that the subsequent high field measurements (described below) were carried out in a region relatively remote from the Curie temperature.

3.2. High Voltage Schering Bridge Measurements

At relatively low field levels (~ 100 V mm^{-1}), dielectric property measurements made using the high voltage Schering bridge showed an excellent correlation with the conventional LCR bridge measurements, as shown in Table 2. Both the dielectric permittivity and loss increased significantly as the applied field was increased to 500 V mm^{-1}; ε_r' increased from 1290 to 1640 (i.e. by a factor of 1.3) over this range of field strengths, while tan δ increased by a factor of 10, from 0.003 to 0.036. These increases in the dielectric coefficients as a function of field strength can be attributed to an increasing ferroelectric domain wall contribution, as discussed by several authors[11,12]. From studies of the ageing behaviour of Fe-doped PZT, Herbiet et al. concluded that the domain wall contribution to ε_r' at 80 °C, measured at low fields, was around 18% for a freshly de-aged sample[13]. This was found to reduce to 9 % after ageing for 1000 min. In contrast, the loss (represented either as ε_r" or tan δ) was assumed to be entirely due to the domain wall motion i.e. the intrinsic ionic contribution to ε_r' was assumed to be essentially loss-free. During ageing, ε_r" was found to decrease by a factor of

approximately 0.6 over a period of 1000 minutes as the domain wall motion was increasingly restricted.

In the present case, the ε_r" and tan δ values measured at low fields were rather low since the specimens had been poled and aged for a period of at least 1 month prior to the tests. As the applied field increased, both ε_r' and ε_r" increased significantly, suggesting an enhanced domain wall contribution as noted above. If it is assumed that the ionic contribution to ε_r' is essentially loss-free, then it is possible to obtain an estimate of this value by plotting ε_r' vs. ε_r" and extrapolating to zero loss, as was done by Herbiet et al. for their dielectric ageing measurements[13]. Such a procedure yields a value of around 1250, as shown in fig. 4.

3.2. P-E Hysteresis Measurements

Typical applied field and induced current waveforms obtained during the P-E hysteresis measurements are presented in fig. 5. For these studies, 2 sinusoidal voltage cycles were applied, which resulted in a current waveform leading the voltage by approximately 90°, as expected from simple AC circuit theory. The current waveform was nearly sinusoidal for applied fields below 100 V mm^{-1}, but began to show an increasing distortion as the field was increased. The corresponding P-E loops are shown in fig. 6. Here, the almost linear behaviour obtained at a field of 100 V mm^{-1} is clearly evident (fig. 6(a)). Increasing field strength was found to give rise to a splitting of the current peaks and the appearance of slim, constricted P-E loops, as shown in figs. 5(b) and 6(b) respectively. This type of behaviour shows some similarity to high field (E_0 ~ 4 kV mm^{-1}) measurements reported in the literature for unpoled hard ferroelectrics, where it is supposed that domain wall pinning effects act to oppose polarisation changes in either sense[14]. The increasing asymmetry of the current waveforms and the slight shift of the P-E loop along the electric field axis are both indications of the internal bias field in these poled materials, which becomes more clearly evident at field strengths of around 2 kV mm^{-1}, as reported previously[15].

Therefore, it can be observed that for poled hard PZT ceramics driven at field levels in this intermediate region (100 to 1000 V mm^{-1}), the domain wall pinning effects act to oppose polarisation changes either parallel or antiparallel to the overall direction of remanent polarisation. In contrast, high field measurements on similar materials usually indicate a

much stronger opposition to polarisation changes opposite to that of the stabilised, aged state i.e. the P-E loops exhibit a large shift along the field axis but not a constriction. These differences in behaviour can be understood qualitatively by recognising that in this intermediate field region there was little change in the overall state of remanent polarisation, since the maximum polarisation change observed in the present study (1.5 μC cm^{-2} at 0.9 kV mm^{-1}) was only 4 % of that measured at high fields.

This effect is illustrated by superimposing one of the P-E loops obtained in the present work on a similar measurement conducted in the high field region[15], as shown in fig. 7. It is concluded that the slim, constricted P-E loops obtained in the intermediate field region (100 to 1000 V mm^{-1}) are a result of small scale domain wall oscillations about an average (stabilised) position rather than the bulk ferroelectric switching which occurs at higher fields.

The effective dielectric coefficients derived from the P-E loops were similar to those found from the high voltage bridge measurements, as shown in Table 3. Again, the ε_r' vs. ε_r" plot (fig. 8) yielded a near linear relationship, with an extrapolated intrinsic ionic contribution to ε_r' of 1310. This was slightly higher than the value of 1250 deduced from the high voltage bridge measurements.

3.3. Fourier Analysis of Voltage and Current Waveforms

FFT analyses yielded similar values for the dielectric coefficients as those reported above, although some minor differences were noted. For these measurements, it was found necessary to analyse a relatively large number of cycles (typically greater than 20) in order to obtain a reasonable resolution in the frequency domain. Therefore, it was not possible to employ just 2 measurement cycles, as was described in section 3.2. Preliminary measurements were conducted by analysing 20 cycles of current and voltage data over a time period up to 1 hour after first application of the field. In this study, increases of the order of 3% were observed in ε_r' over a time period up to 10 minutes. Beyond this, the measured values appeared to stabilise; therefore, a time period of 10 minutes for application of the field prior to recording of the data was chosen as providing a reproducible procedure for subsequent measurements.

A comparison of the resulting ε_r' values with those obtained from the high field bridge and P-E measurements is shown in fig. 9. It is apparent that the FFT analysis yielded values which were around 10% higher than those derived from the other methods, although the overall trend as a function of field strength was similar. Unfortunately, the loss values derived from the FFT analysis exhibited a relatively large scatter due to poor resolution of the phase angle (Table 4). It is anticipated that this could be improved by analysing a larger number of measurement cycles. However, this would probably necessitate the use of a higher frequency signals in order to achieve a reasonable measurement time. This particular aspect was not pursued further in the present work and is an obvious topic for future studies.

A typical FFT analysis, recorded using an applied field of 200 V mm^{-1}, is presented in fig. 10(a); the fundamental component at approximately 1 Hz is clearly evident in this figure. Higher frequency harmonics at integral multiples of the fundamental frequency became apparent as the applied field was increased above 500 V mm^{-1}, as shown in fig. 10(b). The presence of these harmonics is a useful indication of increasing dielectric non-linearity, as illustrated below.

Non-linear dielectric behaviour can be represented by additional (field-dependent) terms in ε_r' [16] :

$$\varepsilon_r'(E) = \varepsilon_r'(0) + \alpha E + \beta E^2 + \ldots \tag{7}$$

$$\therefore \quad P = \varepsilon_0(\varepsilon_r'(0)E + \alpha E^2 + \beta E^3 + \ldots) \tag{8}$$

If we represent the sinusoidal electric field as an exponential term i.e. $E = E_0 e^{j\omega t}$, then the generation of higher frequency harmonics in the current waveform is easily shown :

$$I = A\frac{dP}{dt} = A\varepsilon_0 E_0(\varepsilon_r'(0)j\omega e^{j\omega t} + 2\alpha j\omega e^{2j\omega t} + 3\beta j\omega e^{3j\omega t} + \ldots) \tag{9}$$

$$\therefore \quad I = A\varepsilon_0 E_0(\varepsilon_r'(0)\omega e^{j(\omega t+\frac{\pi}{2})} + 2\alpha\omega e^{j(2\omega t+\frac{\pi}{2})} + 3\beta\omega e^{j(3\omega t+\frac{\pi}{2})} + \ldots) \tag{10}$$

Therefore, it is evident that the growth of higher frequency harmonics in the current waveform provides a means of quantifying the degree of dielectric non-linearity through the magnitudes of the coefficients α, β etc. Furthermore, the magnitudes of the harmonic components were found to increase reproducibly and in a similar manner to the dielectric loss

as the field strength was increased, as shown in fig. 11. This is not altogether unexpected, since both the dielectric loss and non-linearity have their origin in ferroelectric domain wall motion. The occurrence of harmonics in the current waveform potentially provides an ideal means of monitoring non-linearity and loss in practical high power piezoelectric transducers, since the magnitudes of these components could be measured quickly and with high precision using a DSP (Digital Signal Processor) based system.

4. Conclusions

Several different measurement methods were investigated for characterising the dielectric properties of hard PZT ceramics under applied electric fields in the range 100 to 1000 V mm^{-1}. Each of these methods showed that the dielectric permittivity and loss increased significantly as a function of field level, the greatest increase (by a factor of 10 or more) being evident in the loss. These increases in the dielectric coefficients were presumed to arise as a result of an increasing contribution from ferroelectric domain wall motion. ε_r' vs ε_r" plots were constructed using the data derived from high voltage Schering bridge and P-E hysteresis measurements; intrinsic ionic contributions to ε_r' of approximately 1250 and 1310 respectively were derived by extrapolating to zero loss. Fourier analysis indicated the presence of harmonic components in the current waveform, which can be used to provide a quantitative measure of dielectric non-linearity.

Acknowledgements

The authors would like to thank DRA (Holton Heath) for financial support.

References

1. T. Tanaka, "Piezoelectric Devices in Japan", Ferroelectrics **40**, 176-187 (1982).
2. R.E. Newnham and G.R. Ruschau, "Smart Electroceramics", J. Am. Ceram. Soc. **74**, 463-80 (1991).
3. D. Berlincourt, "Piezoelectric Ceramic Compositional Development", J. Acoust. Soc. Am. **91**, 3034-3040 (1992).

4. “Piezoelectric Ceramic Products”, Product Literature, Morgan Matroc Ltd. (Unilator Division, Ruabon, UK).
5. K. Uchino, “Electrostrictive Actuators : Materials and Applications”, Am. Ceram. Soc. Bull. **65**, 647-652 (1986).
6. P.V. Lambeck and G.H. Jonker, “The Nature of Domain Stabilisation in Ferroelectric Perovskites”, J. Phys. Chem. Solids **47**, 453-461 (1986).
7. G. Arlt and H. Neumann, “Internal Bias in Ferroelectric Ceramics : Origin and Time Dependence”, Ferroelectrics **87**, 109-120 (1988).
8. J.L. Butler, K.D. Rolt and F. Tito, “Piezoelectric Ceramic Mechanical and Electrical Stress Study”, J. Acoust. Soc. Am. **96**, 1914-1917 (1994).
9. P. Gerthsen, K.H. Hardtl and N.A. Schmidt, “Correlation of Mechanical and Electrical Losses in Ferroelectric Ceramics”, J. Appl. Phys. **51**, 1131-1134 (1980).
10. K.H. Hardtl, “Electrical and Mechanical Losses in Ferroelectric Ceramics”, Ceramics International **8**, 121-127 (1982).
11. H-J. Hagemann, “Loss Mechanisms and Domain Stabilisation in Doped $BaTiO_3$”, J. Phys. C. : Solid State Phys. **11**, 3333-3344 (1978).
12. S. Li, W. Cao and L.E. Cross, “The Extrinsic Nature of Nonlinear Behaviour Observed in Lead Zirconate Titanate Ferroelectric Ceramic”, J. Appl. Phys. **69**, 7219-7224 (1991).
13. R. Herbiet, H. Tenbrook and G. Arlt, “The Ageing Behaviour of the Complex Material Parameters ε, d and s in Ferroelectric PZT Ceramics”, Ferroelectrics **76**, 319-326 (1987).
14. K. Carl and K.H. Hardtl, “Electrical After-Effects in $Pb(Ti,Zr)O_3$ Ceramics”, Ferroelectrics **17**, 473-486 (1978).
15. D.A. Hall and P.J. Stevenson, “Field-Induced Destabilisation of Hard PZT Ceramics”, Ferroelectrics **187**, 23-37 (1996).
16. U. Robels, Ch. Zadon and G. Arlt, “Linearisation of Dielectric Nonlinearity by Internal Bias Fields”, Ferroelectrics **133**, 163-168 (1992).

Tables

Table 1. Summary of typical room temperature dielectric and piezoelectric coefficients for Ferroperm type PZ26 ceramic.

ε_r	tan δ	Q_m	k_p	k_t
1300	0.003	>1000	0.54	0.38

Table 2. High Voltage Capacitance Bridge Measurements of Dielectric Properties

E_0	ε_r'	tan δ	ε_r''
100	1288	0.0036	4.6
200	1330	0.0074	9.8
300	1410	0.0147	20.7
400	1502	0.0229	34.4
500	1643	0.0355	58.3

Table 3. Field-dependence of dielectric properties derived from P-E measurements

E_0	ε_r'	tan δ	ε_r''
100	1336	0.005	6.7
200	1359	0.005	6.8
300	1391	0.011	15
400	1445	0.018	26
500	1509	0.026	39
600	1570	0.034	53
700	1660	0.044	73
800	1739	0.049	85
900	1809	0.057	103
1000	1870	0.062	115

Table 4. Field-dependence of dielectric properties derived from FFT analysis

E_0	ε_r'	tan δ	ε_r''
100	1468	0.021	30
200	1523	0.005	7
300	1592	0.023	36
400	1661	0.037	61
500	1754	0.036	63
600	1908	0.042	80
700	1988	0.056	111
800	2112	0.042	88
900	2188	0.045	98
1000	2272	0.089	202

List of Figures

Tables

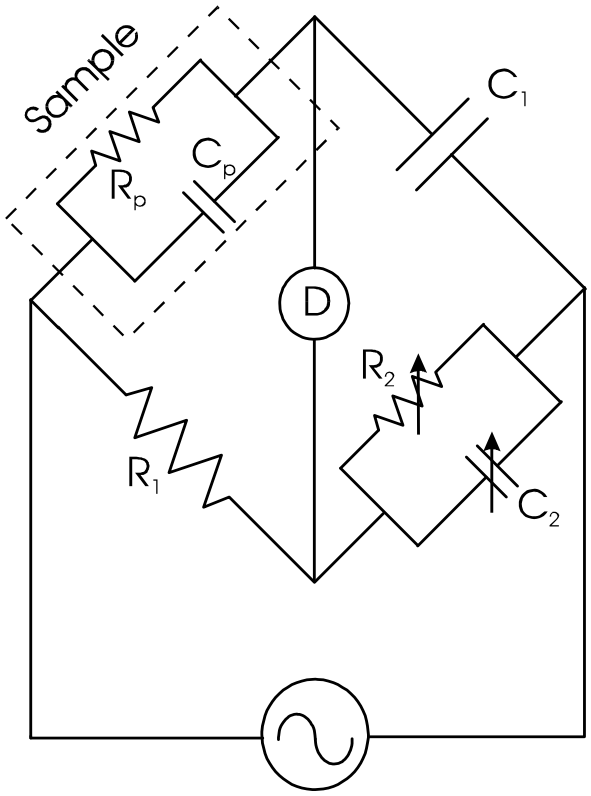

Fig. 1. Outline of Schering bridge circuit.

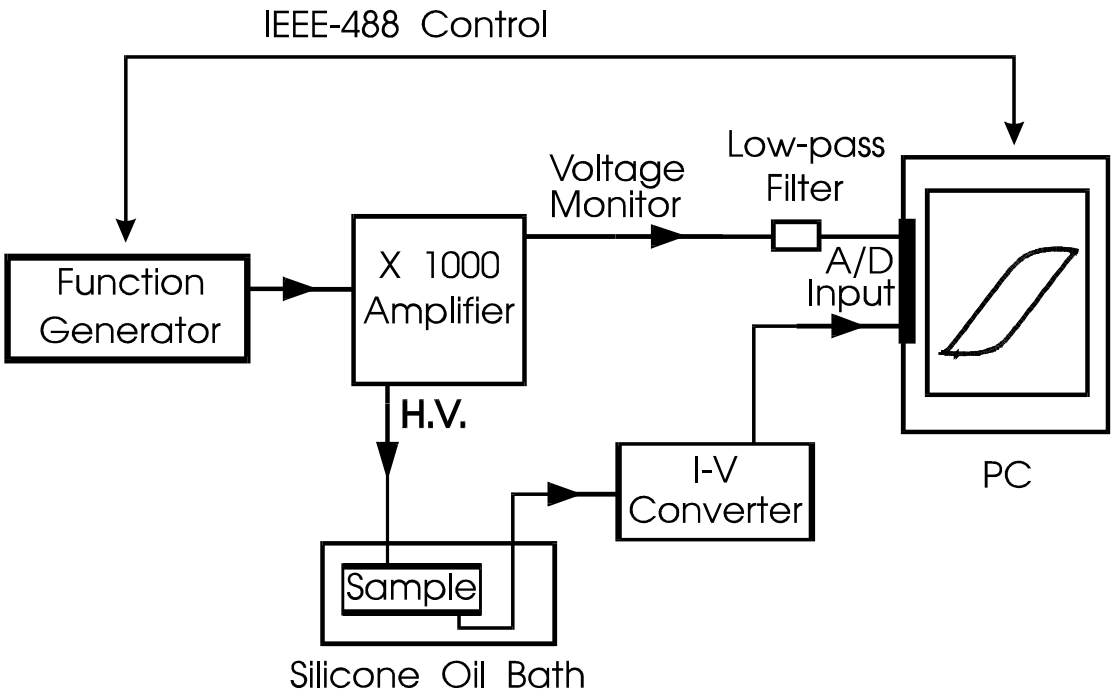

(a)

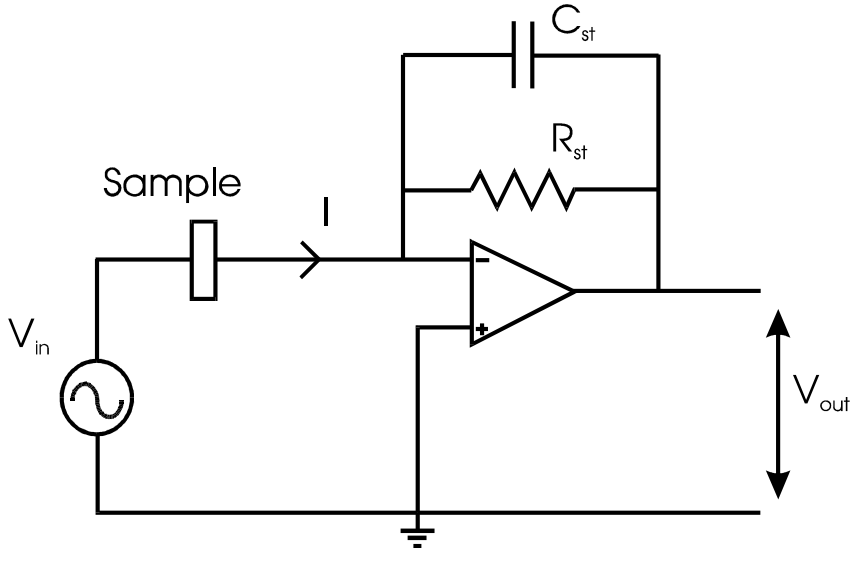

(b)

Fig. 2 (a) P-E measurement setup, (b) detail of I-V Converter.

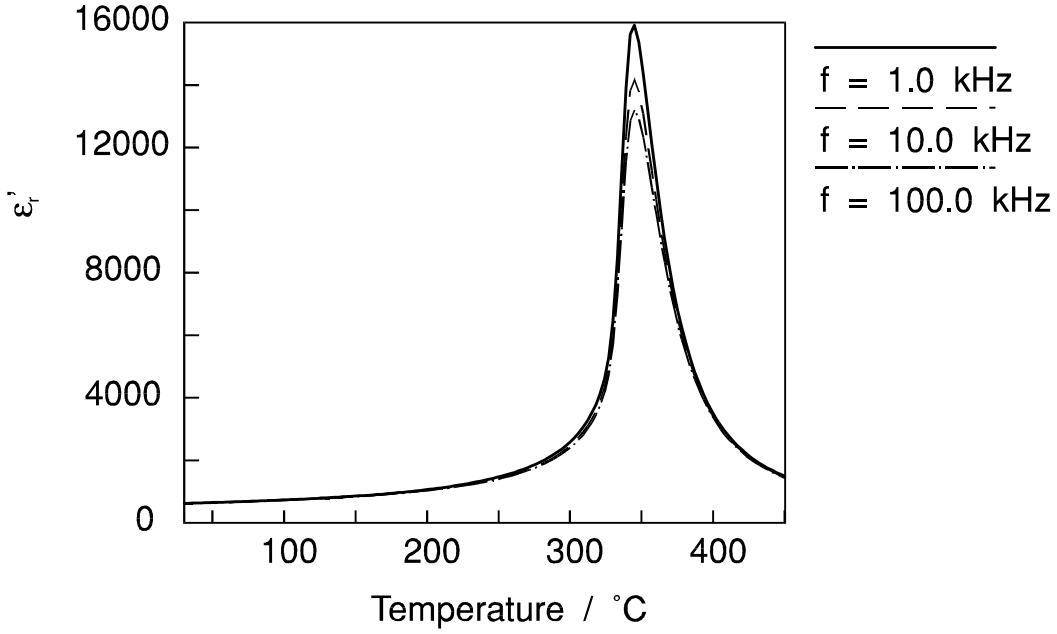

(a)

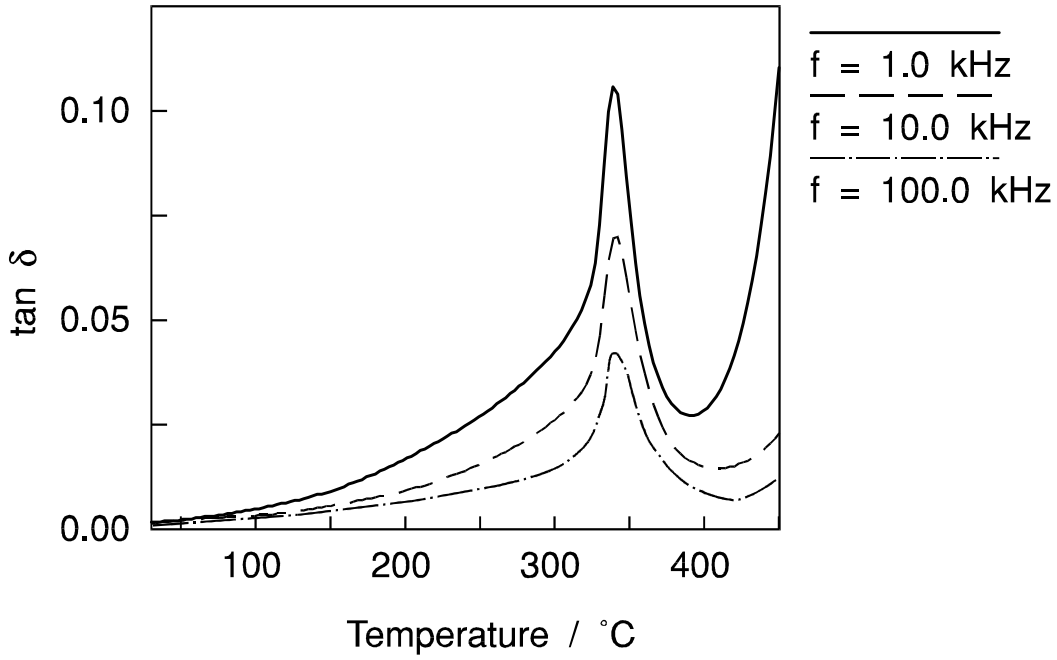

(b)

Fig. 3. Temperature dependence of low field dielectric coefficients; (a) ε_r' and (b) tan δ.

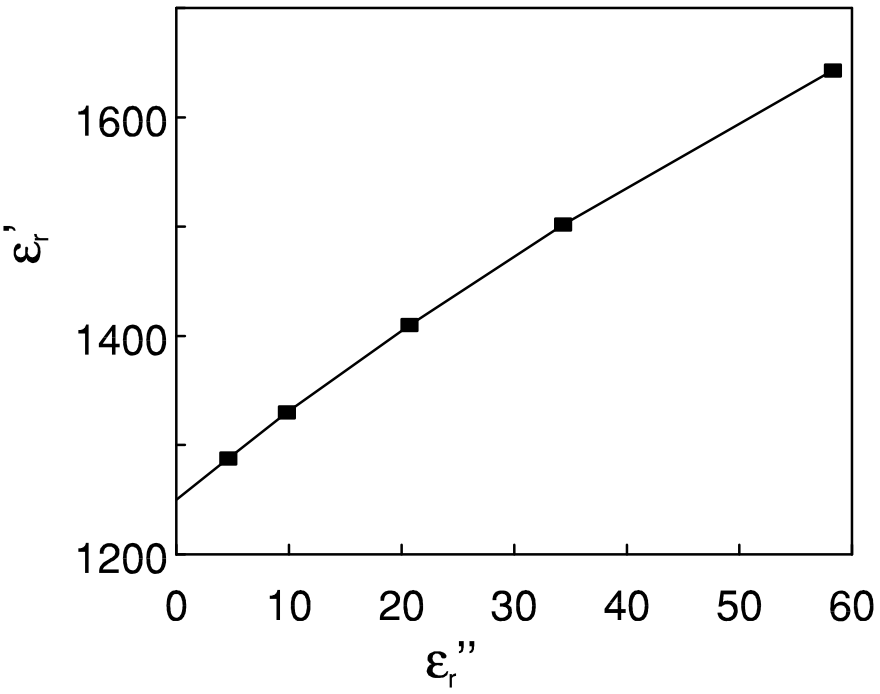

Fig. 4. ε_r' vs ε_r'' plot constructed using high field bridge data.

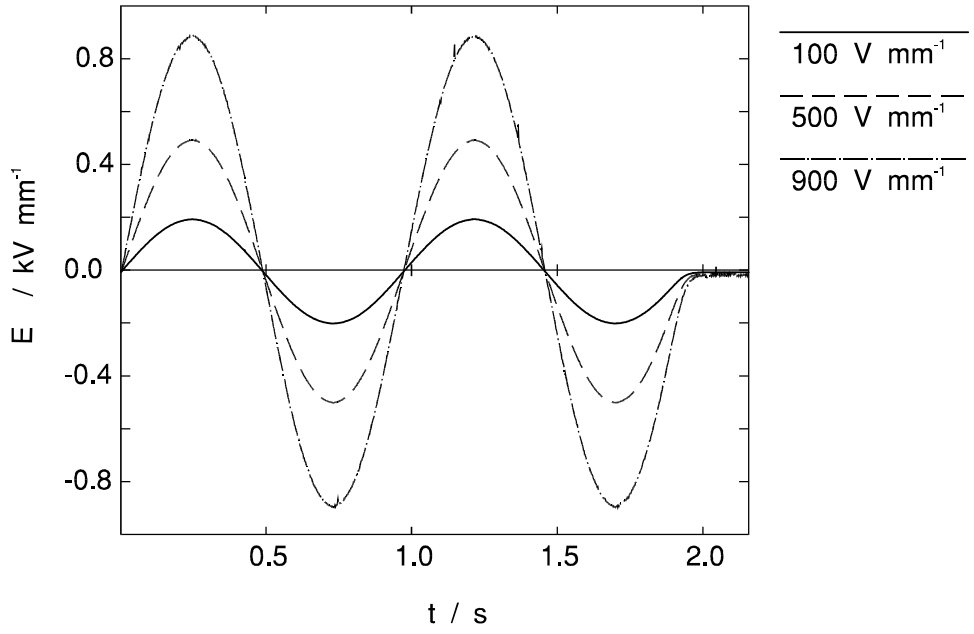

(a)

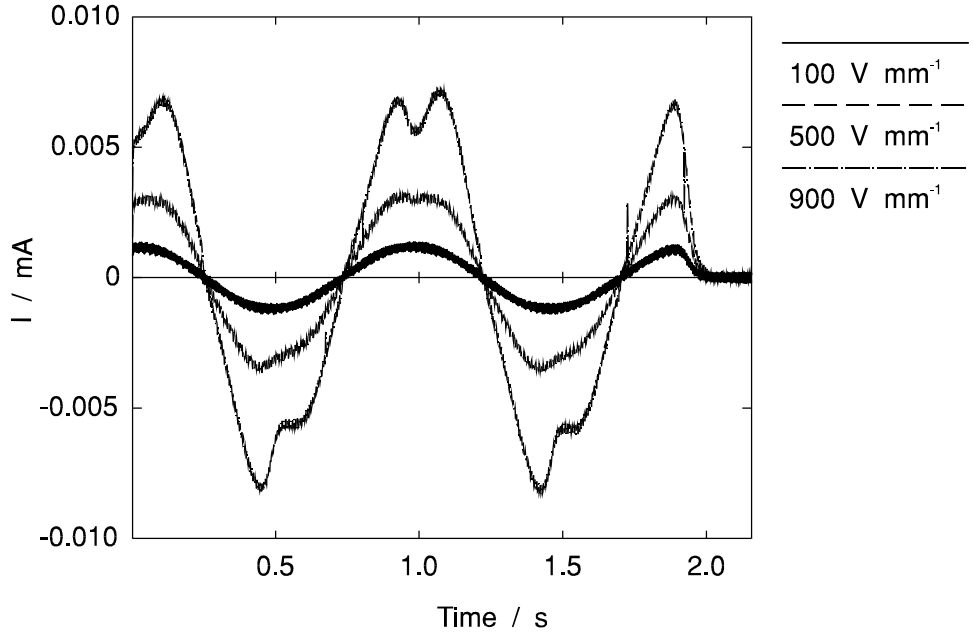

(b)

Fig. 5. Typical (a) applied field and (b) induced current waveforms recorded during P-E measurements.

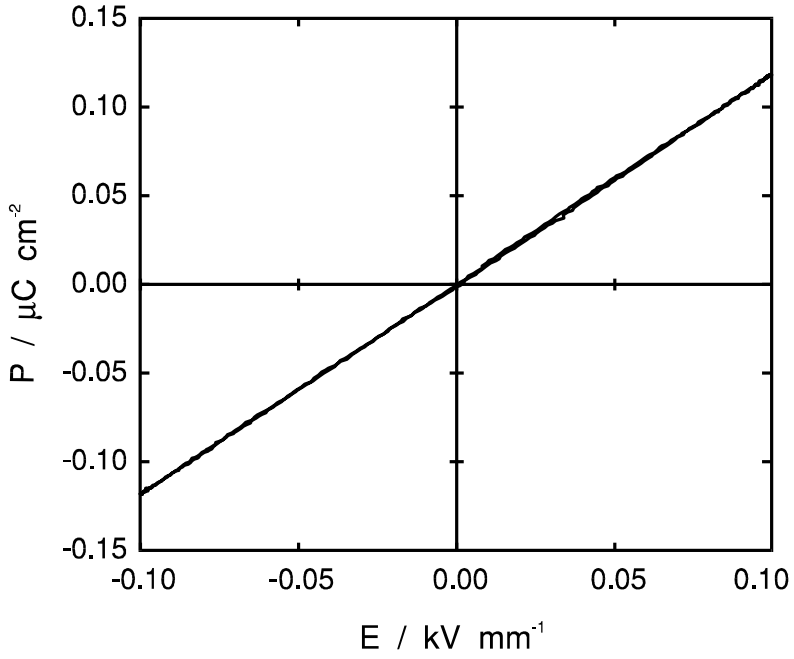

(a)

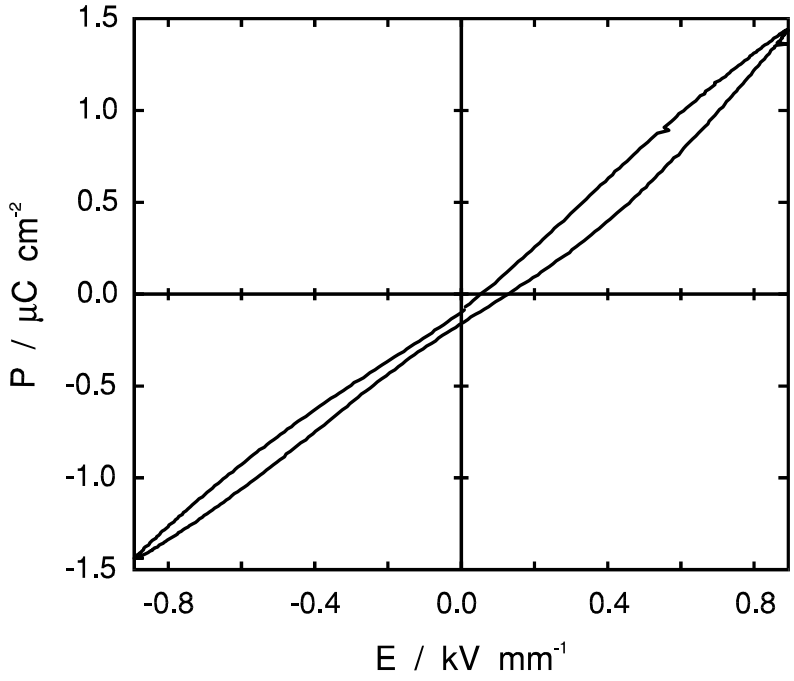

(b)

Fig. 6. Typical P-E hysteresis loops measured at fields of (a) 100 V mm^{-1} and (b) 900 V mm^{-1}.

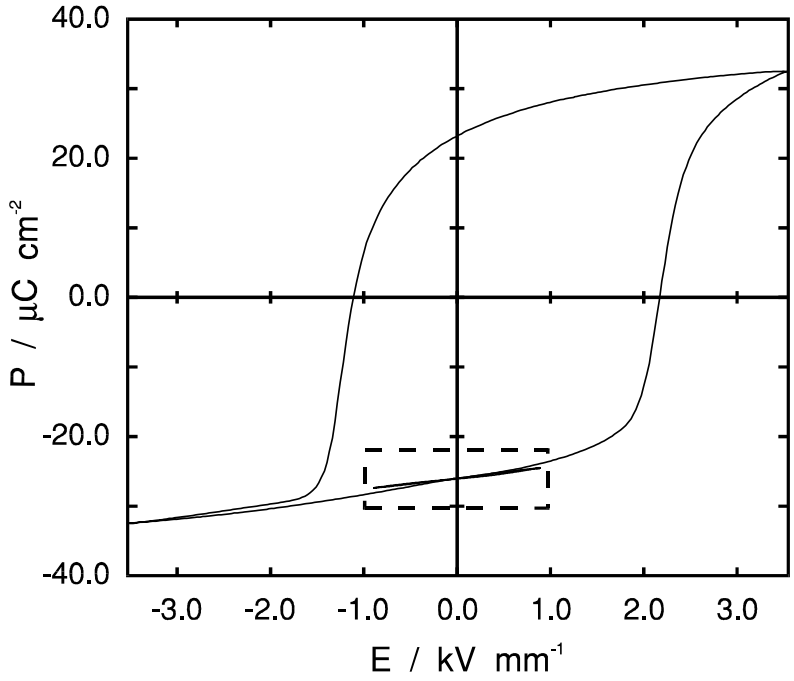

Fig. 7. Comparison of P-E loops measured at fields of 900 V mm^{-1} (present study) and 3.5 kV mm^{-1} [15].

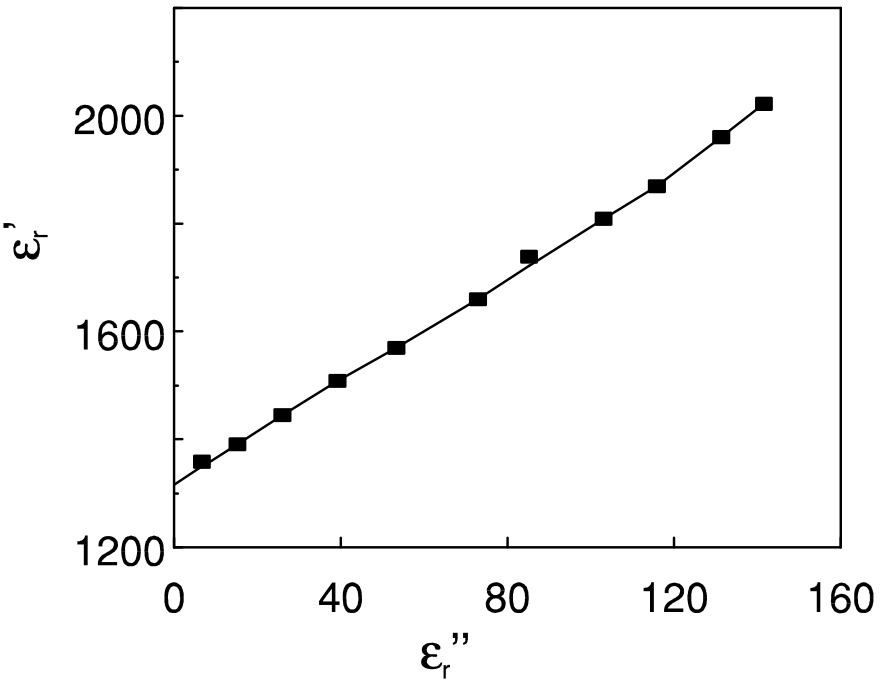

Fig. 8. ε_r' vs ε_r'' plot constructed using P-E hysteresis data.

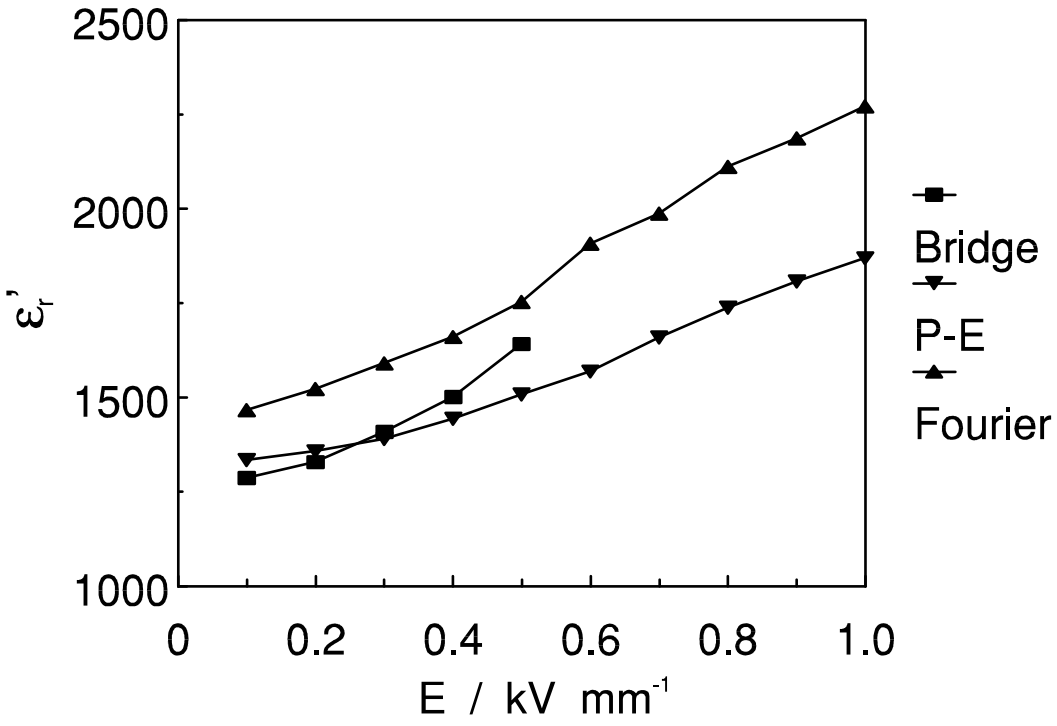

Fig. 9. Comparison of ε_r' values obtained using different measurement methods.

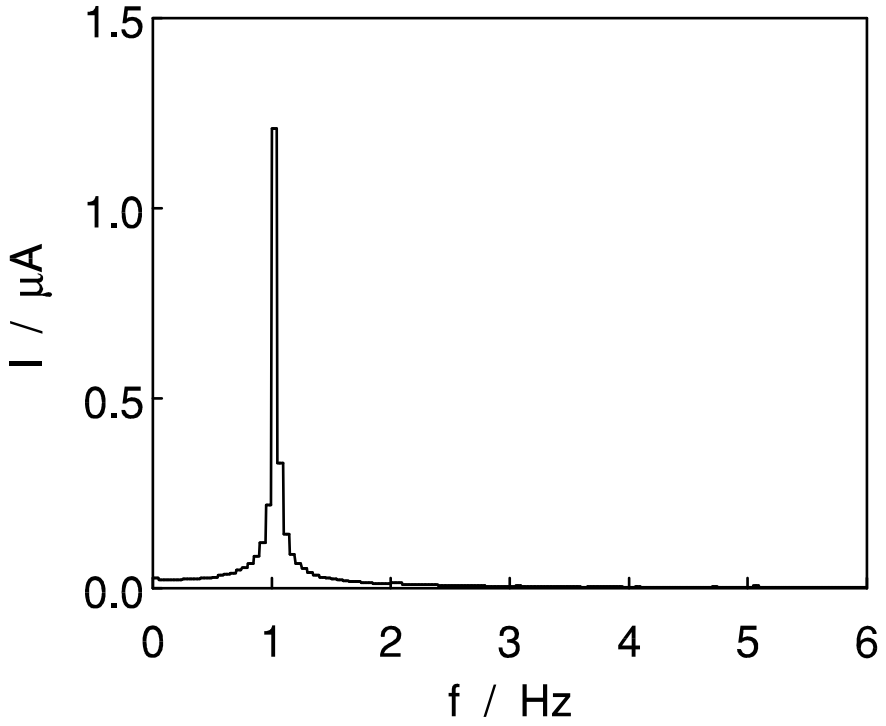

(a)

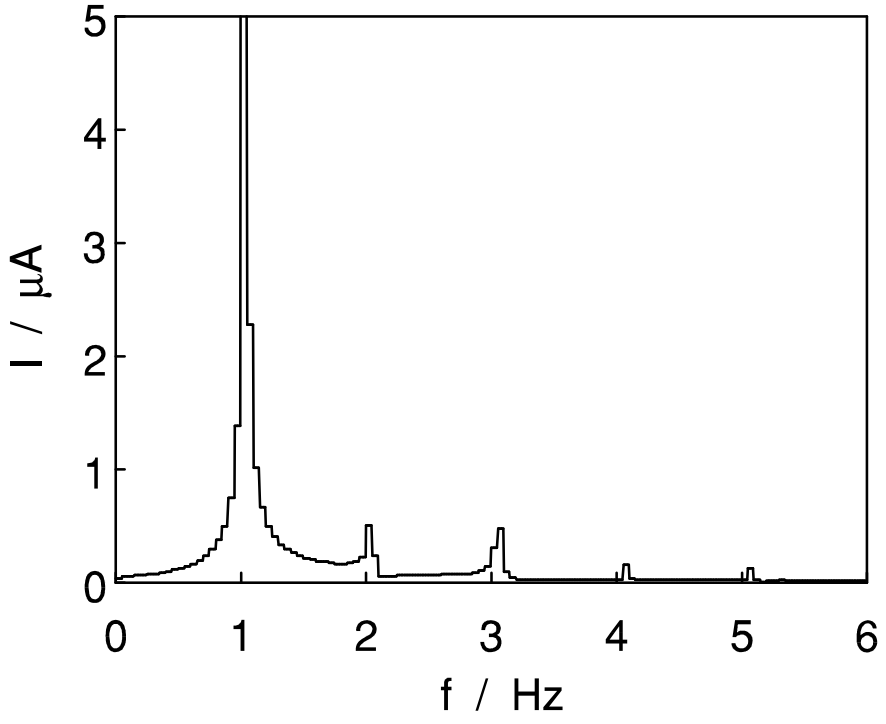

(b)

Fig. 10. FFT analyses of current waveform produced at fields of (a) 200 V mm^{-1} and (b) 900 V mm^{-1}

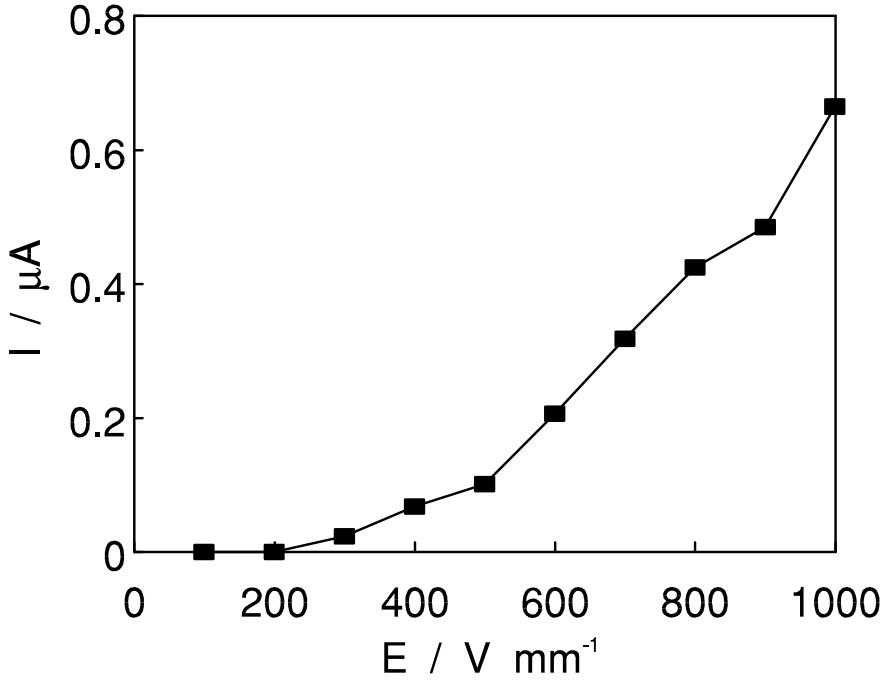

Fig. 11. Growth in the magnitude of the 3 Hz current harmonic with increasing field strength.